Thermochimica Acta 497 (2010) 7–13

Contents lists available at ScienceDirect

Thermochimica Acta

journal homepage: www.elsevier.com/locate/tca

Application of Neumann–Kopp rule for the estimation of heat capacity of mixed oxides

J. Leitner[a,*], P. Voňka[b], D. Sedmidubský[c,d], P. Svoboda[e]

[a] Department of Solid State Engineering, Institute of Chemical Technology Prague, Technická 5, 166 28 Prague 6, Czech Republic
[b] Department of Physical Chemistry, Institute of Chemical Technology Prague, Technická 5, 166 28 Prague 6, Czech Republic
[c] Department of Inorganic Chemistry, Institute of Chemical Technology Prague, Technická 5, 166 28 Prague 6, Czech Republic
[d] European Commission, JRC, Institute for Transuranium Elements, Postbox 2340, D-76125 Karlsruhe, Germany
[e] Department of Condensed Matter Physics, Faculty of Mathematics and Physics, Charles University, Ke Karlovu 5, 120 00 Prague 2, Czech Republic

ARTICLE INFO

Article history:
Received 27 January 2009
Received in revised form 4 August 2009
Accepted 7 August 2009
Available online 14 August 2009

Keywords:
Mixed oxides
Heat capacity
Estimation
Neumann–Kopp rule

ABSTRACT

The empirical Neumann–Kopp rule (NKR) for the estimation of temperature dependence of heat capacity of mixed oxide is analyzed. NKR gives a reasonable estimate of C_{pm} for most mixed oxides around room temperature, but at both low and high temperatures the accuracy of the estimate is substantially lowered. At very low temperatures, the validity of NKR is shown to be predominantly determined by the relation between the characteristic Debye and Einstein temperatures of a mixed oxide and its constituents. At high temperatures, the correlation between their molar volumes, volume expansion coefficients and compressibilities takes the dominance. In cases where the formation of a mixed oxide is not accompanied by any volume change, the difference between dilatation contributions to heat capacity of a mixed oxide and its constituents is exclusively negative. It turns out that in the high-temperature range, where the contribution of harmonic lattice vibrations approached the $3NR$ limit, $\Delta_{ox}C_p$ assumes negative values. For more complex oxides whose heat capacity has contributions from terms such as magnetic ordering, electronic excitations, the applicability of NKR is only restricted to lattice and dilatation terms.

1. Introduction

Binary and mixed oxides[1] are currently being employed in a number of technical applications such as structural materials, protection coatings (thermal barrier coatings) and functional materials in electronics. Heat capacity at constant pressure is one of the essential thermophysical characteristics determining the thermal behavior of a given material. The temperature dependence of heat capacity is also used in calculations of enthalpy and entropy changes with temperature changes, such as evaluation of $\Delta_f H(298.15\,\mathrm{K})$ and $S_m(298.15\,\mathrm{K})$ from high-temperature equilibrium measurements or in calculation of $G_m(T)$ from the thermodynamic data for $T = 298.15$ K, in phase diagram computations.

Although heat capacity is a relatively easily accessible property from the experimental point of view and can be measured for solids over a broad temperature range from $T \to 0$ up to their melting temperature, C_{pm} data are still not available for a large number of mixed oxides, both stoichiometric compounds and solid solutions. In such cases, heat capacity and its temperature dependence are usually estimated on the basis of the empirical Neumann–Kopp rule (NKR) [1].

NKR has been, for instance, recently applied in the following cases of mixed oxides:

- High-temperature measurements of electromotive force (EMF) of galvanic cells involving solid electrolytes and $\Delta_f H(298.15\,\mathrm{K})$ and $S_m(298.15\,\mathrm{K})$ evaluation for $Nd_2Ir_2O_7$, $Nd_6Ir_2O_{13}$ (975–1450 K) [2], $AgRhO_2$ (980–1235 K) [3], $NdMnO_3$, $NdMn_2O_5$ (925–1400 K) [4], $CaRuO_3$ (815–1053 K) [5] or Sr_2RuO_4, $Sr_3Ru_2O_7$ (951–1098 K) [6].
- Phase equilibria calculations and phase diagram mapping, e.g. for the systems $BaO–TiO_2$ [7], $BaO–SrO–TiO_2$ [8], $Al_2O_3–La_2O_3$ [9].
- Interpretation of measured C_{pm} data of mixed oxides such as $BaUO_3$ [10], $Ba_2Te_3O_8$, $Ba_3Te_2O_9$ [11] Dy_2TiO_5, Gd_2TiO_5 [12] and solid solutions $(U,Th)O_2$ [13] or $(U,Pu)O_2$ [14].
- Evaluation of thermal conductivity $k = \alpha\rho c_p$ from the measured thermal diffusivity α and density ρ of $LaAlO_3$, $Sm_2Zr_2O_7$ and $Eu_2Zr_2O_7$ [15].

Based on the comparison of experimental values of $C_{pm}(298.15\,\mathrm{K})$ and the values estimated using NKR for more than 300 mixed oxides, Leitner et al. [16] corroborated the appli-

---

* Corresponding author.
E-mail address: jindrich.leitner@vscht.cz (J. Leitner).

[1] Both stoichiometric compounds (e.g. Ca_2SiO_4) and solid solutions (e.g. $(Ca_{1-x}Sr_x)O$ or $Bi(Nb_{1-x}Ta_x)O_4$) are referred to as mixed oxides in the following text.

doi:10.1016/j.tca.2009.08.002

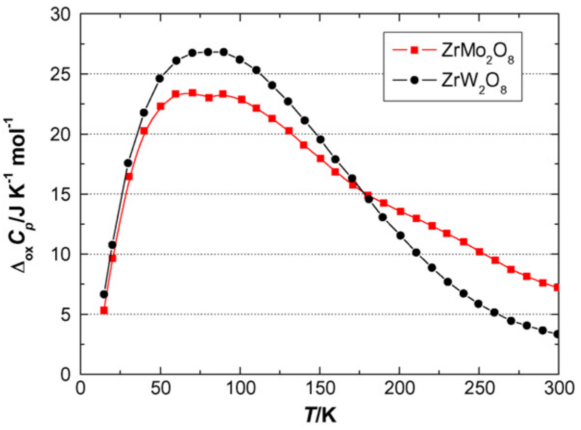

Fig. 1. Temperature dependence of $\Delta_{ox}C_p$ for $ZrMo_2O_8$ (■) and ZrW_2O_8 (●) [17].

cability of NKR in the vicinity of ambient temperature showing that NKR provides an estimate with an average error bar of 3.3%. However, in a number of other studies NKR was found to give a much larger error at both low and very high temperatures. Stevens et al. [17,18] measured the temperature dependence of C_{pm} for ZrW_2O_8, $ZrMo_2O_8$ [17] and Zn_2GeO_4 [18] in the range 0.5–400 K and found substantial positive deviations from NKR exhibiting a maximum in a given temperature interval and then, a decrease towards room temperature (see Fig. 1). A similar behavior was observed by Tojo et al. for solid solutions ZrO_2–Y_2O_3 [19,20] and CeO_2–ZrO_2 [21] (13–300 K). Further examples of mixed oxides revealing either positive or negative departures from NKR below room temperature are referred by Qiu and White [22]. On the other hand, the results of Richet and Fiquet [23] demonstrate that in the case of $MgAl_2O_4$, Mg_2SiO_4 and $CaMgSi_2O_6$ minerals, the difference between the experimental C_{pm} and NKR increases gradually from ambient temperature reaching 4–6% at $T \approx 2000$ K.

In the present work, we focus on a detailed analysis of NKR and its applicability for the prediction of temperature dependence of the heat capacity of mixed oxides. An attention is in particular drawn to the high-temperature region where an accurate estimation of C_{pm} is crucial for the evaluation of calorimetric and equilibrium measurement results as well as for calculations of phase equilibria in mixed oxide systems.

2. Neumann–Kopp rule

Neumann–Kopp rule has been postulated more than 140 years ago on the basis of an extensive collection of experimental C_{pm} data compiled by Kopp [1] and other researchers, in particular by Neumann and Renault, for solid substances. The rule (in original terms the law) was first presented by Kopp in the following form: "*Each element* (*in the solid state*) *has essentially the same specific or atomic heat in compounds as it has in the free state*". Let us note that a *compound* is here referred to as a synonym to *solid body* which involves both stoichiometric compounds and solid solutions and, furthermore, only the C_{pm} values around ambient temperature are considered.

The heat capacities of most of the elements known at that time were equal, in agreement with Dulong–Petit rule (law), to a value 26.7 J K^{-1} mol^{-1} (6.4 cal K^{-1} mol^{-1}). However, for some elements (S, P, Si, B or C) Kopp recommended lower values obtained either directly from the measured values of the respective heat capacities or from the C_{pm} data of some compounds formed by these elements. Using this approach (from C_{pm} data of a compound and other elements forming this compound) hypothetical values of heat capacities in a solid state were assessed for those elements which occur in a gaseous state at normal conditions (H, O and F).

Mathematically, NKR can be expressed as follows: If a solid compound $A_aB_bC_c$ is formed from solid elements A, B and C by a reaction:

$$a\,\mathrm{A(s)} + b\,\mathrm{B(s)} + c\,\mathrm{C(s)} = \mathrm{A}_a\mathrm{B}_b\mathrm{C}_c\mathrm{(s)} \qquad (1)$$

then, according to NKR, the corresponding heat capacity reads:

$$C_{pm}(\mathrm{A}_a\mathrm{B}_b\mathrm{C}_c,\mathrm{s}) = a\,C_{pm}(\mathrm{A,s}) + b\,C_{pm}(\mathrm{B,s}) + c\,C_{pm}(\mathrm{C,s}) \qquad (2)$$

Note that NKR cannot be generally considered as a simple additive scheme based on calculating a compound (molecule) property as a sum of the respective properties of real elements forming this compound, which is used for instance when calculating molar weights from the atomic weights. The heat capacities of H, O and F reported by Kopp should be rather considered as contributions which have been evaluated by a mathematical approach and cannot be experimentally determined. NKR thus represents a combination of an additive and contribution method. Later on, a number of empirical contribution methods has been proposed that can be applied for the estimation of heat capacities of solids, e.g. for binary solid oxides [24,25], mixed oxides [16] or oxide glasses [26,27].

From the beginning, NKR has been a subject of a considerable interest for researchers. Meyer [28] demonstrated that NKR was satisfied for those solid compounds whose molar volume was approximately equal to a stoichiometric sum of atomic volumes of elements forming that compound. According to his findings, $C_{pm}(\mathrm{compound}) > \sum C_{pat}(\mathrm{elements})$ if $V_m(\mathrm{compound}) > \sum V_{at}(\mathrm{elements})$ and vice versa [28]. Nevertheless, the general validity of the above relation was later disproved [29] and contradictory behavior was found for some other compounds.

For the prediction of heat capacities of complex compounds NKR was modified accordingly [16,22]. To estimate C_{pm} of a ternary solid compound $A_aB_bC_c$ being formed upon a reaction of binary compounds AC_{c1} and BC_{c2}:

$$a\,\mathrm{AC}_{c1}\mathrm{(s)} + b\,\mathrm{BC}_{c2}\mathrm{(s)} = \mathrm{A}_a\mathrm{B}_b\mathrm{C}_c\mathrm{(s)} \qquad (3)$$

we can assume:

$$C_{pm}(\mathrm{A}_a\mathrm{B}_b\mathrm{C}_c,\mathrm{s}) = a\,C_{pm}(\mathrm{AC}_{c1},\mathrm{s}) + b\,C_{pm}(\mathrm{BC}_{c2},\mathrm{s}) \qquad (4)$$

This modification not only increases the reliability of the estimation [22], but also extends the applicability to those cases, when an element does not occur in solid state at a given temperature and pressure (e.g. complex halides, oxides, nitrides, etc.).

3. Temperature dependence of molar heat capacity

The molar heat capacity of a solid at constant pressure can be expressed as a sum of several contributions [30]:

$$C_{pm} = C_{ph} + C_{dil} + C_{others} \qquad (5)$$

where C_{ph} represents the contribution of lattice vibrations (phonons), C_{dil} stands for lattice dilatation and C_{others} comprises further contributions (conduction electrons, excitations of localized electrons, ordering changes upon second order phase transitions or formation of vacancies). The latter term, or rather a sum of all other contributions, is not necessarily involved in all solids and will not be considered hereafter. Although the formation of various defects such as oxygen vacancies is very common in oxides, the heat capacity contribution from vacancies, C_{vac}, is not considered in further analysis which is confined to stoichiometric ideal crystals. In general, C_{vac} is positive and increases with temperature as $C_{vac} \approx (E_{vac}/k_BT)^2 \exp(-E_{vac}/k_BT)$, where E_{vac} is the energy of vacancy formation. Considering the typical values of E_{vac}, this term becomes important at temperatures close to the melting point [30].

The phonon contribution C_{ph} can be expressed in terms of heat capacity described within harmonic crystal approximation C_{har} and an additional correction to internal anharmonicity of vibrational modes, C_{anh}:

$$C_{\mathrm{ph}} = C_{\mathrm{har}} + C_{\mathrm{anh}} \tag{6}$$

The harmonic part assumes a general form:

$$C_{\mathrm{har}} = R\int_0^{\nu_{\max}} \left(\frac{h\nu}{k_{\mathrm{B}}T}\right)^2 \frac{e^{h\nu/k_{\mathrm{B}}T}}{[e^{h\nu/k_{\mathrm{B}}T}-1]^2}\, g(\nu)\,\mathrm{d}\nu \tag{7}$$

where ν is a specific phonon frequency and $g(\nu)$ is the phonon density of states (PDOS). As the real phonon spectrum consists of three acoustic branches and $3N-3$ optical bands, where N is the number of atoms per formula unit (or more appropriately per primitive unit cell) of a given substance, it is convenient to approximate it by one triply degenerate Debye mode simulating the acoustic modes and $3N-3$ Einstein modes representing the optical modes:

$$C_{\mathrm{har}} = 9R\left(\frac{T}{\Theta_{\mathrm{D}}}\right)^3 \int_0^{x_{\mathrm{D}}} \frac{x^4 e^x}{(e^x-1)^2}\,\mathrm{d}x + R\sum_{i=1}^{3N-3} \frac{x_{\mathrm{E}i}^2 \cdot e^{x_{\mathrm{E}i}}}{[e^{x_{\mathrm{E}i}}-1]^2} \tag{8}$$

Here $x_{\mathrm{D}} = \theta_{\mathrm{D}}/T$ and $x_{\mathrm{E}i} = \theta_{\mathrm{E}i}/T$ with θ_{D} and $\theta_{\mathrm{E}i}$ being the characteristic Debye and Einstein temperatures which can be considered as free parameters. To reduce the number of parameters to be fitted, the Einstein modes can be grouped so that the essential features of the phonon spectrum and their weights are reproduced. If the particular phonon spectrum is unknown the Einstein modes are usually grouped by trial-and-error to achieve the best fit with the experimental heat capacity. Nevertheless, such an approach is not only suitable for the analysis of experimental data. Since the characteristic temperatures reveal clear trends within the isostructural series of compounds reflecting the dependence of lattice dynamics on atomic masses and strengths of individual bonds, the hybrid Debye–Einstein model can be used to estimate the heat capacities in cases the experimental data are not available.

The correction for internal anharmonicity has been thoroughly discussed by Gillet et al. [31–35]. In a simplified form this correction could be considered as

$$C_{\mathrm{ph}} = \sum_i C_{\mathrm{har},i}(1-2a_iT) \tag{9}$$

where a_i is an anharmonic parameter of the ith vibrational mode with frequency ν_i defined as

$$a_i = \left(\frac{\partial \ln \nu_i}{\partial T}\right)_V \tag{10}$$

The anharmonic parameters are rare in literature. They can be obtained from high temperature—high pressure Raman and IR spectroscopy. In general these values are negative in order of $(1\text{–}5) \times 10^{-5}\,\mathrm{K}^{-1}$. It means that the anharmonic contributions are significant at temperatures around 1000 K and higher. For example, C_{anh} = 1.5%, 4.6% and 8.2% (from C_{ph}) for Ca_2GeO_4 at 1000, 1500 and 2000 K, respectively [31]. A detailed evaluation of C_{pm} and p–V–T data for Mg_2SiO_4 [36] allows to calculate C_{anh} as well as C_{dil} terms in the broad temperature range (Fig. 2).

For the dilatation term representing the difference between the molar heat capacities at constant pressure and constant volume, the relation:

$$C_{\mathrm{dil}} = C_{pm} - C_{V\mathrm{m}} = \frac{TV_{\mathrm{m}}\alpha^2}{\beta} = -T\frac{(\partial V_{\mathrm{m}}/\partial T)_p^2}{(\partial V_{\mathrm{m}}/\partial p)_T} \tag{11}$$

is often applied including the experimental quantities—molar volume, V_{m}, isothermal coefficient of volume expansion, α, and isobaric compressibility, β. Both the dilatation term and the internal anharmonic correction are particularly relevant in high-temperature range, where the harmonic part approaches the Dulong–Petit limit $3NR$. Hence, for the low temperature limit where only the low frequency acoustic modes are active, we can simplify the first Debye term in Eq. (8) and write:

$$T \to 0 \Rightarrow C_{pm} \to C_{\mathrm{har}} \to \frac{12\pi^4 R}{5}\left(\frac{T}{\theta_{\mathrm{D}}}\right)^3 \tag{12}$$

while in the high-temperature limit each term in Eq. (8) approaches the value of R ($3R$ for triply degenerate Debye mode) and the Dulong–Petit limit is thus applicable. Hence:

$$\frac{T}{\theta_{\mathrm{D}}} \gg 1 \Rightarrow C_{pm} = C_{\mathrm{har}} + C_{\mathrm{anh}} + C_{\mathrm{dil}} \to 3NR + C_{\mathrm{anh}} + \frac{TV_{\mathrm{m}}\alpha^2}{\beta} \tag{13}$$

It follows from the above relations (12) and (13) that at very low temperatures the NKR validity is predominantly conditioned by a relation between the Debye and Einstein temperatures of a mixed oxide and its constituents, while at high temperatures the relations between V_{m}, α and β as well as the internal anharmonic corrections are relevant.

4. NKR prediction of C_{pm} temperature dependence

Let us consider a formation of a mixed oxide from binary oxides AO_a and BO_b described by the equation (assuming 1 mol of a mixed oxide and x_{A}, x_{B} being the normalized constitution coefficients or molar fractions of a stoichiometric phase or a solid solution, respectively):

$$x_{\mathrm{A}}\,AO_a(s) + x_{\mathrm{B}}\,BO_b(s) = A_{x_{\mathrm{A}}}B_{x_{\mathrm{B}}}O_z(s),$$
$$z = x_{\mathrm{A}}a + x_{\mathrm{B}}b, \quad x_{\mathrm{A}} + x_{\mathrm{B}} = 1 \tag{14}$$

It follows from Eqs. (12) and (14) that at very low temperatures, where no other but the low frequency acoustic modes are populated, NKR is satisfied whenever the relation:

$$\theta_{\mathrm{D,AB}} = \frac{\theta_{\mathrm{D,A}}\theta_{\mathrm{D,B}}}{(x_{\mathrm{B}}\theta_{\mathrm{D,A}}^3 + x_{\mathrm{A}}\theta_{\mathrm{D,B}}^3)^{1/3}} \tag{15}$$

holds for the pertinent Debye temperatures [30,37]. However, in real mixed oxides the Debye temperature is not only weighted by constituent coefficients but also by atomic masses of cations whose vibrations predominantly contribute the low frequency modes. For instance, in the phonon spectrum (PDOS) of $BaZrO_3$ (Fig. 3) calculated by direct method [38,39] the large peak centered at ∼2.5 THz representing the acoustic phonons has a prevailing Ba-character

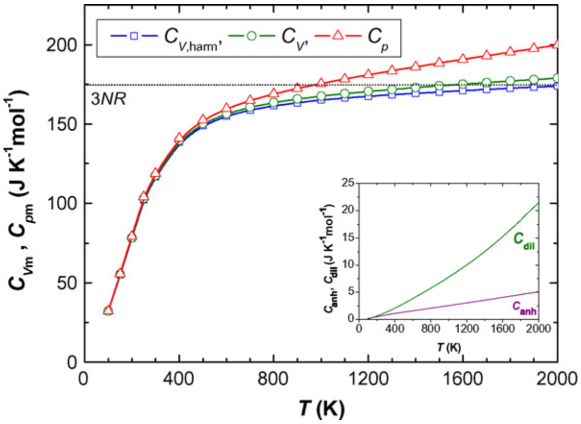

Fig. 2. Temperature dependence of C_{pm} and $C_{V\mathrm{m}}$ for Mg_2SiO_4 [36]. C_{anh} and C_{dil} contributions are shown in the inset.

Table 1
Debye and Einstein temperatures fitted on the experimental heat capacity data. All modes are triply degenerate for the former three compounds while the Einstein modes of the latter two have the degeneracies 2 and 1, respectively.

Substance	Θ_D (K)	Θ_{E1} (K)	Θ_{E2} (K)	Θ_{E3} (K)	Θ_{E4} (K)
$BaZrO_3$	182 ± 3	185 ± 4	393 ± 22	461 ± 27	846 ± 12
$SrZrO_3$	209 ± 2	222 ± 4	465 ± 10	465 ± 10	844 ± 11
ZrO_2	354.4 ± 0.2	522.5 ± 0.4	874.9 ± 0.5	–	–
BaO	177.8 ± 0.3	286.9 ± 0.9	521 ± 2	–	–
SrO	271.8 ± 0.6	400 ± 2	592 ± 4	–	–

(80%) which entails the corresponding Debye temperature is only slightly higher than that in BaO and much lower than in ZrO_2 (see Table 1). Moreover, as apparent from Fig. 3 the low frequency spectrum of BaO reveals two distinct branches (noticeable as two different peaks located at 2 and 4 THz) while $BaZrO_3$ shows only a single peak. The different dispersion of acoustic branches in alkaline earth (and presumably also other highly ionic) binary oxides and in the respective mixed oxides is manifested by a positive peak in the difference PDOS (shown in the inset of Fig. 3) and gives rise to a very common positive divergence from NKR at low temperatures resulting also in positive values of the entropies of formation from binary oxides, $\Delta_{ox}S(298.15\,\text{K})$, at ambient temperature.

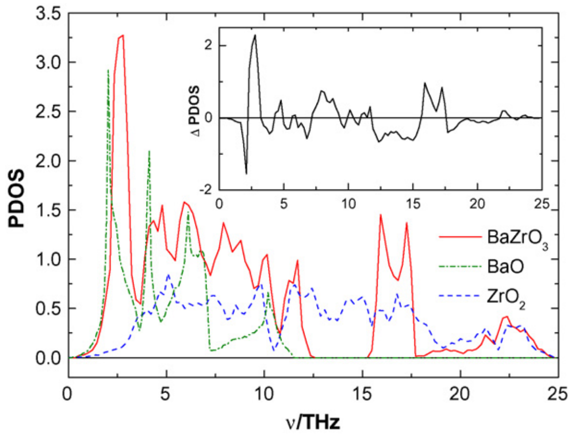

Fig. 3. Phonon density of states (PDOS) of $BaZrO_3$ (solid line) and the constituent oxides (dashed lines) calculated using phonon [38] and VASP [39] programs. The difference PDOS is plotted in the inset.

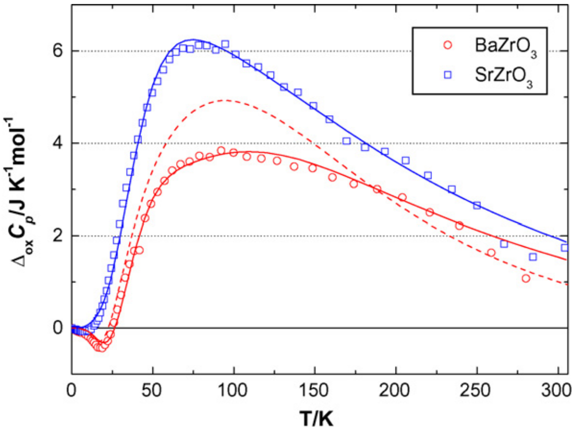

Fig. 4. Temperature dependence of $\Delta_{ox}C_p$ for $SrZrO_3$ (□) and $BaZrO_3$ (○). The solid lines represent the Debye–Einstein fits and the dashed line corresponds to the heat capacity of $BaZrO_3$ calculated from phonon density of states (Fig. 3).

This characteristic behavior is demonstrated in Fig. 4 for two selected mixed oxides as $\Delta_{ox}C_p(T)$ evaluated from the experimental heat capacity data of $BaZrO_3$ [40], $SrZrO_3$ [40], BaO [41], SrO [41] and ZrO_2 [20]. In addition, the curves calculated from Debye–Einstein fit, Eq. (8), are shown for both oxides and compared with an *ab initio* based $\Delta_{ox}C_p(T)$ dependence calculated for $BaZrO_3$ (Eq. (7) and PDOS from Fig. 3). The fitted characteristic temperatures of Debye–Einstein model (Eq. (8)) for all compounds involved are summarized in Table 1. Note that the observed effect is more pronounced in the case of $SrZrO_3$ which exhibits even lower Debye temperature compared to SrO. Moreover, the calculated phonon band structure of SrO shows even larger splitting of acoustic branches than BaO.

Let us now focus on the high-temperature region, where $C_{\rm har}$ is saturated at the Dulong–Petit limit. Neglecting the anharmonic corrections $C_{\rm anh}$, NKR is then satisfied if

$$\Delta C_{\rm dil} = C_{\rm dil,AB} - x_A C_{\rm dil,A} - x_B C_{\rm dil,B} = \frac{TV_{\rm m,AB}\alpha_{\rm AB}^2}{\beta_{\rm AB}} - x_A\frac{TV_{\rm m,A}\alpha_{\rm A}^2}{\beta_{\rm A}} - x_B\frac{TV_{\rm m,B}\alpha_{\rm B}^2}{\beta_{\rm B}} = 0 \qquad (16)$$

Let first assume a zero volume change accompanying the reaction (14), i.e. $\Delta V_{\rm AB} = \Delta_{\rm ox}V = 0$ for a stoichiometric phase or $\Delta V_{\rm AB} = \Delta V^{\rm M} = 0$ for a solid solution. In analogy to NKR for heat capacities, Eq. (4), we can write for molar volume:

$$V_{\rm m,AB} = x_A V_{\rm m,A} + x_B V_{\rm m,B} \qquad (17)$$

Note that in the case of solid solutions Eq. (17) is in contradiction to Vegard's law [42] postulating the additivity of lattice cell parameters. The validity of the relation (17) for the stoichiometric mixed oxides cannot be explicitly anticipated. Nevertheless, empirical methods for the estimation of unit cell volumes of solid organic and organometallic [43] as well as inorganic [44] substances as sums of average volume contributions of the constituent elements or ions, respectively, have been proposed, which is indeed in agreement with (17). It can be proved (see Appendix A) that in such a case:

$$\Delta C_{\rm dil} = -Tx_A x_B \frac{\beta_A\beta_B}{\beta_{\rm AB}}\frac{V_{\rm m,A}V_{\rm m,B}}{V_{\rm m,AB}}\left(\frac{\alpha_A}{\beta_A} - \frac{\alpha_B}{\beta_B}\right)^2 \le 0 \qquad (18)$$

NKR is thus completely or nearly satisfied if the quotients α_i/β_i for both constituents of a mixed oxide do not differ substantially. If this is not the case, the heat capacity of the mixed oxide reveals negative deviations from NKR.

Given the condition (17) is not satisfied, we express the molar volume of a mixed oxide as

$$V_{\rm m,AB} = x_A V_{\rm m,A} + x_B V_{\rm m,B} + \Delta V_{\rm AB} \qquad (19)$$

whereas $\Delta V_{\rm AB}$ can attain both positive and negative values. Based on the consideration shown in Appendix A we find out that the sign of $\Delta C_{\rm dil}$ is now also affected by the values of $\Delta\alpha_{\rm AB}$ and $\Delta\beta_{\rm AB}$ (see relations (A14) and (A15) for definitions). For the combination $\Delta\alpha_{\rm AB} < 0$ and $\Delta\beta_{\rm AB} > 0$ a mixed oxide will exhibit the negative deviations from NKR, while for other combinations this cannot be determined *a priori*.

Table 2
Molar volume at $T = 298.15$ K ($V_m(298)$), coefficient of thermal expansion (α) and compressibility (β) for selected oxides.

Substance	$V_m(298)$ ($m^3\ mol^{-1}$)	α (K^{-1})	β (Pa^{-1})
$BaZrO_3$	4.457×10^{-5}	2.27×10^{-5} [47]	7.86×10^{-12} [48]
$SrZrO_3$	4.162×10^{-5}	2.65×10^{-5} [47]	2.96×10^{-12} [48]
ZrO_2	2.118×10^{-5}	2.69×10^{-5} [49]	5.35×10^{-12} [50]
BaO	2.681×10^{-5}	3.87×10^{-5} [51]	1.45×10^{-11} [52]
SrO	2.069×10^{-5}	4.17×10^{-5} [51]	1.10×10^{-11} [52]

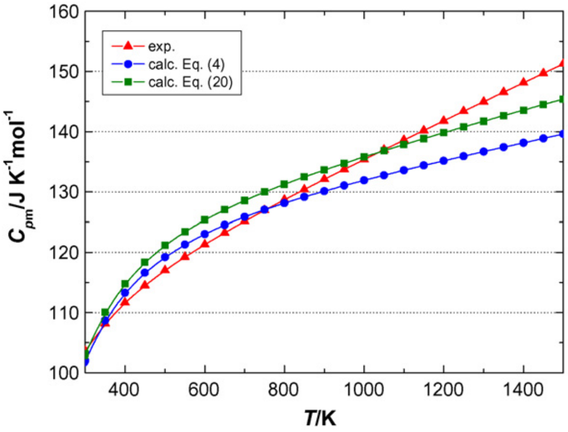

Fig. 5. Temperature dependence of C_{pm} for $SrZrO_3$. Experimental data [46] (▲), calculated according to NKR, Eq. (4) (●), calculated according to Eq. (20) (■)

As the difference between dilatation terms for a mixed oxide and the stoichiometric sum of constituent binary oxides was recognized as the crucial part of $\Delta_{ox}C_p$ at high temperatures, an improved procedure for estimation of the heat capacity of mixed oxides is considered bellow. The ΔC_{dil} term (Eq. (16)) is simply added to the right side of Eq. (4) which for the mixed oxides $A_{x(A)}B_{x(B)}O_z(s)$ (Eq. (14)) is read:

$$C_{pm}(A_{x_A}B_{x_B}O_z) = x_A C_{pm}(AO_a) + x_B C_{pm}(BO_b) + \Delta C_{dil} \tag{20}$$

This procedure is now illustrated considering the high-temperature heat capacity of $SrZrO_3$ and $BaZrO_3$. The C_{pm} data for binary oxides SrO, BaO and ZrO_2 were taken from thermodynamic tables [45], for the mixed oxides, $SrZrO_3$ and $BaZrO_3$, the data from [46] were used. Other parameters necessary for ΔC_{dil} calculations are summarized in Table 2. It should be noted that relevant data from other sources are slightly different in some cases. Figs. 5 and 6 show the temperature dependences of the heat capacity of $SrZrO_3$ and $BaZrO_3$ calculated according to NKR (Eq. (4)) and using the proposed procedure (Eq. (20)) in comparison with experimental data. It is obvious that the new method improves the C_{pm} prediction for positive ($SrZrO_3$) as well as for negative ($BaZrO_3$) deviations from the NKR.

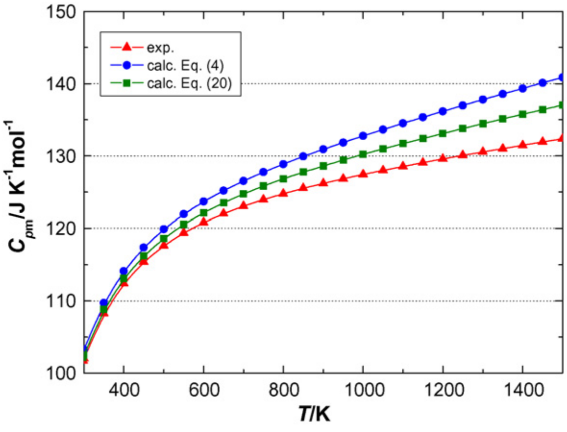

Fig. 6. Temperature dependence of C_{pm} for $BaZrO_3$. Experimental data [46] (▲), calculated according to NKR, Eq. (4) (●), calculated according to Eq. (20) (■).

5. Conclusions

Based on the performed analysis, we can conclude that the empirical NKR is applicable for the heat capacities of solid substances around ambient temperature namely in those cases when lattice vibration and dilatation terms are the only two contributions of a mixed oxide and the corresponding binary oxides. At markedly low temperatures, the nonzero value of $\Delta_{ox}C_p$ is related to the difference in the lattice contribution to the heat capacity of a mixed oxide due to a change of vibrational frequencies upon formation of mixed oxide. A detailed analysis of phonon spectrum $BaZrO_3$ perovskite, taken as an example case, revealed the most striking difference between the low frequency acoustic modes of $BaZrO_3$ and BaO which gives rise to a positive divergence from NKR. The observed difference bears apparently relation to different bonding characteristics (coordination number and site symmetry) of the large cation in the mixed and binary oxide. This tendency is even accentuated when going to lighter alkaline earth analogues as documented on an analysis of $SrZrO_3$ in terms of Debye–Einstein model.

At substantially higher temperatures, the departure of $\Delta_{ox}C_p$ from zero is due to the difference between the dilatation terms as a result of molar volume contraction or expansion as well as the variation of thermal expansion and compressibility coefficients. A simple modification of the NKR for the estimation of C_{pm} of mixed oxides was suggested which consist in addition ΔC_{dil} term to the stoichiometric sum of the heat capacities of the constituent binary oxides.

For those oxides, whose heat capacity has contributions from other terms (associated, e.g. with a magnetic ordering), NKR can be only applied to their lattice contribution, as it has been demonstrated on some stoichiometric mixed oxides such as $LaFeO_3$ [53] or $ErFeO_3$ and $HoFeO_3$ [54].

Acknowledgments

This work was supported by the Ministry of Education of the Czech Republic (Research Projects No. MSM6046137302 and No. MSM6046137307) and the Czech Science Foundation (grant No. 104/07/1209).

Appendix A.

Derivation of a relation for the difference in dilatation contributions $\Delta C_{dil} = C_{dil,AB} - x_A C_{dil,A} - x_B C_{dil,B}$:

$$\Delta C_{dil} = \frac{TV_{m,AB}\alpha_{AB}^2}{\beta_{AB}} - x_A \frac{TV_{m,A}\alpha_A^2}{\beta_A} - x_B \frac{TV_{m,B}\alpha_B^2}{\beta_B} \tag{A1}$$

Let us first consider the case:

$$\Delta V_{\mathrm{AB}} = V_{\mathrm{m,AB}} - x_{\mathrm{A}} V_{\mathrm{m,A}} - x_{\mathrm{B}} V_{\mathrm{m,B}} = 0 \tag{A2}$$

It follows from the definition α and β coefficients ($y_{\mathrm{A}} = x_{\mathrm{A}} V_{\mathrm{m,A}}/V_{\mathrm{m,AB}}$ and $y_{\mathrm{B}} = x_{\mathrm{B}} V_{\mathrm{m,B}}/V_{\mathrm{m,AB}}$) that:

$$\alpha_{\mathrm{AB}} = \frac{x_{\mathrm{A}} V_{\mathrm{m,A}}}{V_{\mathrm{m,AB}}}\alpha_{\mathrm{A}} + \frac{x_{\mathrm{B}} V_{\mathrm{m,B}}}{V_{\mathrm{m,AB}}}\alpha_{\mathrm{B}} = y_{\mathrm{A}}\alpha_{\mathrm{A}} + y_{\mathrm{B}}\alpha_{\mathrm{B}} \tag{A3}$$

and

$$\beta_{\mathrm{AB}} = \frac{x_{\mathrm{A}} V_{\mathrm{m,A}}}{V_{\mathrm{m,AB}}}\beta_{\mathrm{A}} + \frac{x_{\mathrm{B}} V_{\mathrm{m,B}}}{V_{\mathrm{m,AB}}}\beta_{\mathrm{B}} = y_{\mathrm{A}}\beta_{\mathrm{A}} + y_{\mathrm{B}}\beta_{\mathrm{B}} \tag{A4}$$

With respect to Eq. (A2) it follows that $y_{\mathrm{A}} + y_{\mathrm{B}} = 1$.

The Eq. (A1) is divided by temperature T:

$$\frac{\Delta C_{\mathrm{dil}}}{T} = V_{\mathrm{m,AB}}\frac{\alpha_{\mathrm{AB}}^2}{\beta_{\mathrm{AB}}} - x_{\mathrm{A}} V_{\mathrm{m,A}}\frac{\alpha_{\mathrm{A}}^2}{\beta_{\mathrm{A}}} - x_{\mathrm{B}} V_{\mathrm{m,B}}\frac{\alpha_{\mathrm{B}}^2}{\beta_{\mathrm{B}}} \tag{A5}$$

and the resulting relation is further arranged into a form:

$$\frac{\Delta C_{\mathrm{dil}}}{T V_{\mathrm{m,AB}}} = \frac{\alpha_{\mathrm{AB}}^2}{\beta_{\mathrm{AB}}} - y_{\mathrm{A}}\frac{\alpha_{\mathrm{A}}^2}{\beta_{\mathrm{A}}} - y_{\mathrm{B}}\frac{\alpha_{\mathrm{B}}^2}{\beta_{\mathrm{B}}} \tag{A6}$$

The relation (A6) is now to be multiplied by a positive quotient $\beta_{\mathrm{AB}}/\alpha_{\mathrm{AB}}{}^2$ and, simultaneously, the second and third term are extended by quotients $y_{\mathrm{A}}/y_{\mathrm{A}}$ and $y_{\mathrm{B}}/y_{\mathrm{B}}$, respectively.

$$\frac{\Delta C_{\mathrm{dil}}}{T V_{\mathrm{m,AB}}}\frac{\beta_{\mathrm{AB}}}{\alpha_{\mathrm{AB}}^2} = 1 - \frac{(y_{\mathrm{A}}(\alpha_{\mathrm{A}}/\alpha_{\mathrm{AB}}))^2}{y_{\mathrm{A}}(\beta_{\mathrm{A}}/\beta_{\mathrm{AB}})} - \frac{(y_{\mathrm{B}}(\alpha_{\mathrm{B}}/\alpha_{\mathrm{AB}}))^2}{y_{\mathrm{B}}(\beta_{\mathrm{B}}/\beta_{\mathrm{AB}})} \tag{A7}$$

Let us define new variables u_{A}, u_{B}, v_{A}, v_{B}

$$y_{\mathrm{A}}\frac{\alpha_{\mathrm{A}}}{\alpha_{\mathrm{AB}}} = u_{\mathrm{A}}, \quad y_{\mathrm{B}}\frac{\alpha_{\mathrm{B}}}{\alpha_{\mathrm{AB}}} = u_{\mathrm{B}}, \quad u_{\mathrm{A}} + u_{\mathrm{B}} = 1 \tag{A8}$$

and

$$y_{\mathrm{A}}\frac{\beta_{\mathrm{A}}}{\beta_{\mathrm{AB}}} = v_{\mathrm{A}}, \quad y_{\mathrm{B}}\frac{\beta_{\mathrm{B}}}{\beta_{\mathrm{AB}}} = v_{\mathrm{B}}, \quad v_{\mathrm{A}} + v_{\mathrm{B}} = 1 \tag{A9}$$

The expression (A7) is then arranged to

$$\frac{\Delta C_{\mathrm{dil}}}{T V_{\mathrm{m,AB}}}\frac{\beta_{\mathrm{AB}}}{\alpha_{\mathrm{AB}}^2} = 1 - \frac{u^2}{v} - \frac{(1-u)^2}{1-v} = F(u, v) \tag{A10}$$

where $u = u_{\mathrm{A}}$, $u_{\mathrm{B}} = 1 - u$, $v = v_{\mathrm{A}}$, $v_{\mathrm{B}} = 1 - v$. The function $F(u, v)$ can be rewritten in a form:

$$F(u, v) = -\frac{(v-u)^2}{v(1-v)} = -v(1-v)\left[\frac{u}{v} - \frac{1-u}{1-v}\right]^2 \le 0 \tag{A11}$$

which provides the evidence that in case $\Delta V_{\mathrm{AB}} = 0$ the value of ΔC_{dil} will never be positive. After substituting for u and v in (A10) we obtain the final formula:

$$\Delta C_{\mathrm{dil}} = -T x_{\mathrm{A}} x_{\mathrm{B}}\frac{\beta_{\mathrm{A}}\beta_{\mathrm{B}}}{\beta_{\mathrm{AB}}}\frac{V_{\mathrm{m,A}} V_{\mathrm{m,B}}}{V_{\mathrm{m,AB}}}\left(\frac{\alpha_{\mathrm{A}}}{\beta_{\mathrm{A}}} - \frac{\alpha_{\mathrm{B}}}{\beta_{\mathrm{B}}}\right)^2 \le 0 \tag{A12}$$

In the general case:

$$\Delta V_{\mathrm{AB}} = V_{\mathrm{m,AB}} - x_{\mathrm{A}} V_{\mathrm{m,A}} - x_{\mathrm{B}} V_{\mathrm{m,B}} \ne 0 \tag{A13}$$

the following relations for α_{AB} and β_{AB} will result:

$$\alpha_{\mathrm{AB}} = y_{\mathrm{A}}\alpha_{\mathrm{A}} + y_{\mathrm{B}}\alpha_{\mathrm{B}} + \frac{1}{V_{\mathrm{m,AB}}}\left(\frac{\partial \Delta V_{\mathrm{AB}}}{\partial T}\right)_p = y_{\mathrm{A}}\alpha_{\mathrm{A}} + y_{\mathrm{B}}\alpha_{\mathrm{B}} + \Delta\alpha_{\mathrm{AB}} \tag{A14}$$

and

$$\beta_{\mathrm{AB}} = y_{\mathrm{A}}\beta_{\mathrm{A}} + y_{\mathrm{B}}\beta_{\mathrm{B}} - \frac{1}{V_{\mathrm{m,AB}}}\left(\frac{\partial \Delta V_{\mathrm{AB}}}{\partial p}\right)_T = y_{\mathrm{A}}\beta_{\mathrm{A}} + y_{\mathrm{B}}\beta_{\mathrm{B}} + \Delta\beta_{\mathrm{AB}} \tag{A15}$$

whereas $y_{\mathrm{A}} + y_{\mathrm{B}} \ne 1$ and the variables $\Delta\alpha_{\mathrm{AB}}$ and $\Delta\beta_{\mathrm{AB}}$ can assume both positive and negative values. Unfortunately, it is not possible to express the difference in dilatation terms in such a form, which would unambiguously show its sign. Nevertheless, the following qualitative reasoning is conceivable: For $\Delta V_{\mathrm{AB}} = 0$ is the expression (A5) never positive. For $\Delta V_{\mathrm{AB}} \ne 0$, only the first term in (A5) will change assuming the form:

$$\begin{aligned} V_{\mathrm{m,AB}}\frac{\alpha_{\mathrm{AB}}^2}{\beta_{\mathrm{AB}}} &= V_{\mathrm{m,AB}}\frac{(y_{\mathrm{A}}\alpha_{\mathrm{A}} + y_{\mathrm{B}}\alpha_{\mathrm{B}} + \Delta\alpha_{\mathrm{AB}})^2}{y_{\mathrm{A}}\beta_{\mathrm{A}} + y_{\mathrm{B}}\beta_{\mathrm{B}} + \Delta\beta_{\mathrm{AB}}} \\ &= \frac{(x_{\mathrm{A}} V_{\mathrm{m,A}}\alpha_{\mathrm{A}} + x_{\mathrm{B}} V_{\mathrm{m,B}}\alpha_{\mathrm{B}} + V_{\mathrm{m,AB}}\Delta\alpha_{\mathrm{AB}})^2}{x_{\mathrm{A}} V_{\mathrm{m,A}}\beta_{\mathrm{A}} + x_{\mathrm{B}} V_{\mathrm{m,B}}\beta_{\mathrm{B}} + V_{\mathrm{m,AB}}\Delta\beta_{\mathrm{AB}}} \end{aligned} \tag{A16}$$

If $\Delta\alpha_{\mathrm{AB}} < 0$ and simultaneously $\Delta\beta_{\mathrm{AB}} > 0$, the fraction $V_{\mathrm{m,AB}}\alpha^2{}_{\mathrm{AB}}/\beta_{\mathrm{AB}}$ will be lower than in the case $\Delta V_{\mathrm{AB}} = 0$ and thus $\Delta C_{\mathrm{dil}} < 0$ (cf. Eq. (A5)). In all other cases the influence of $\Delta\alpha_{\mathrm{AB}}$ and $\Delta\beta_{\mathrm{AB}}$ on the resulting sign of ΔC_{dil} cannot be definitely determined.

References

[1] H. Kopp, Phil. Trans. R. Soc. Lond. 155 (1865) 71.
[2] K.T. Jacob, T.H. Okabe, T. Uda, Y. Waseda, Electrochim. Acta 45 (2000) 1963.
[3] K.T. Jacob, T. Uda, T.H. Okabe, Y. Waseda, J. Chem. Thermodyn. 32 (2000) 1399.
[4] K.T. Jacob, M. Attaluri, K. Fitzner, CALPHAD 26 (2002) 313.
[5] A. Banerjee, R. Prasad, V. Venugopal, J. Alloys Compd. 358 (2003) 321.
[6] A. Banerjee, R. Prasad, V. Venugopal, J. Alloys Compd. 373 (2004) 59.
[7] X. Lu, Z. Jin, CALPHAD 24 (2000) 319.
[8] W. Gong, Z. Jin, CALPHAD 26 (2002) 403.
[9] O. Fabrichnaya, M. Zinkevich, F. Aldinger, Int. J. Mater. Res. 97 (2006) 1495.
[10] T. Matsuda, S. Yamanaka, K. Kurosaki, M. Uno, S. Kobayashi, J. Alloys Compd. 322 (2001) 77.
[11] R. Agarwal, Z. Singh, J. Alloys Compd. 414 (2006) 230.
[12] G. Panneerselvam, R. Venkata Krishnan, M.P. Antony, K. Nagarajan, T. Vasudevan, P.R. Vasudeva Rao, J. Nucl. Mater. 327 (2004) 220.
[13] R. Agarwal, R. Prasad, V. Venugopal, J. Nucl. Mater. 322 (2003) 98.
[14] R. Kandan, R. Babu, K. Nagarajan, P.R. Vasudeva Rao, Thermochim. Acta 472 (2008) 46.
[15] G. Suresh, G. Seenivasan, M.V. Krishnaiah, P. Srirama Murti, J. Alloys Compd. 269 (1998) L9.
[16] J. Leitner, P. Chuchvalec, D. Sedmidubský, A. Strejc, P. Abrman, Thermochim. Acta 395 (2003) 27.
[17] R. Stevens, J. Linford, B.F. Woodfield, J. Boerio-Goates, C. Lind, A.P. Wilkinson, G. Kowach, J. Chem. Thermodyn. 35 (2003) 919.
[18] R. Stevens, B.F. Woodfield, J. Boerio-Goates, M.K. Crawford, J. Chem. Thermodyn. 36 (2004) 349.
[19] T. Tojo, T. Atake, T. Mori, H. Yamamura, J. Therm. Anal. Calorim. 57 (1999) 447.
[20] T. Tojo, T. Atake, T. Mori, H. Yamamura, J. Chem. Thermodyn. 31 (1999) 831.
[21] T. Tojo, H. Kawaji, T. Atake, T. Mori, H. Yamamura, J. Chem. Eng. Data 48 (2003) 1479.
[22] L. Qiu, M.A. White, J. Chem. Educ. 78 (2001) 1076.
[23] P. Richet, G. Fiquet, J. Geophys. Res. 96 (1991) 445.
[24] J. Leitner, P. Chuchvalec, D. Sedmidubský, Chem. Listy 95 (2001) 2.
[25] J. Leitner, D. Sedmidubský, P. Chuchvalec, Ceramics-Silikáty 46 (2002) 29.
[26] P. Richet, Y. Bottinga, Rev. Geophys. 24 (1986) 1.
[27] S.A. Khalimovskaya-Churkina, A.I. Priven, Glass Phys. Chem. 216 (2000) 531.
[28] S. Meyer, Ann. Phys. 2 (1900) 135.
[29] E. van Aubel, Ann. Phys. 4 (1901) 420.
[30] G. Grimvall, Thermophysical Properties of Materials, Elsevier, 1999, pp. 367–368.
[31] P. Gillet, F. Guyot, J.-M. Malezieux, Phys. Earth Planet. Interiors 58 (1989) 141.
[32] P. Gillet, P. Richet, F. Guyot, G. Fiquet, J. Geophys. Res. 96 (1991) 11805.
[33] G. Fiquet, P. Gillet, P. Richet, Phys. Chem. Miner. 18 (1992) 469.
[34] P. Richet, P. Gillet, G. Fiquet, in: S.K. Saxena (Ed.), Thermodynamic Data. Systematics and Estimation, Springer, Berlin, 1992 (Chapter 4).
[35] P. Gillet, Phys. Chem. Miner. 23 (1996) 263.
[36] M.H.G. Jacobs, B.H.W.S. de Jong, Phys. Chem. Miner. 32 (2005) 614.
[37] G.B. Mitra, T. Chattopadhyay, Acta Cryst. A 28 (1972) 179.
[38] K. Parlinski, Softw. Phonon. (2006).
[39] G. Kresse, J. Furthmüller, Phys. Rev. B 54 (1996) 11169.
[40] K. Kurosaki, R.J.M. Konings, F. Wastin, S. Yamanaka, J. Alloys Compd. 424 (2006) 1.
[41] E.H.P. Cordfunke, R.R. van der Laan, J.C. van Miltenburg, J. Phys. Chem. Solids 55 (1994) 77.
[42] K.T. Jacob, S. Raj, L. Rannesh, Int. J. Mater. Res. 98 (2007) 776.
[43] D.W.M. Hofmann, Acta Cryst. B 57 (2002) 489.
[44] L. Glasser, H.D.B. Jenjins, Inorg. Chem. 47 (2008) 6195.
[45] O. Knacke, O. Kubaschewski, K. Hesselmann, Thermochemical Properties of Inorganic Substances, 2nd ed., Springer, Berlin, 1991, p. 21.
[46] M.E. Huntelaar, E.H.P. Cordfunke, R.R. van der Laan, Thermochim. Acta 274 (1996) 101.
[47] M.D. Mathews, E.B. Mirya, A.C. Momin, J. Mater. Sci. Lett. 10 (1991) 305.

[48] S. Yamanaka, K. Kurosaki, T. Maekawa, T. Matsuda, S. Kobayashi, M. Uno, J. Nucl. Mater. 344 (2005) 61.
[49] R.N. Patil, E.C. Subbarao, J. Appl. Cryst. 2 (1969) 281.
[50] M. Iuga, G. Steinle-Neumann, J. Meinhardt, Eur. Phys. J. B 58 (2007) 127.
[51] Z.P. Chang, E.K. Graham, J. Phys. Chem. Solids 38 (1977) 1355.
[52] T. Tsuchiya, K. Kawamura, J. Chem. Phys. 114 (2001) 10086.
[53] S. Stølen, F. Grønvold, H. Brinks, T. Atake, H. Mori, J. Chem. Thermodyn. 30 (1998) 365.
[54] S.C. Parida, S.K. Rakshit, S. Dash, Z. Singh, B.K. Sen, V. Venugopal, J. Solid State Chem. 179 (2006) 2212.